Legal Medicine 61 (2023) 102215

Contents lists available at ScienceDirect

Legal Medicine

journal homepage: www.elsevier.com/locate/legalmed

A novel method to estimate adult age from the lumbar vertebral body using 3D PMCT images in Japanese

Dawa Zangpo [a,b], Kazutake Uehara [c], Katsuya Kondo [d], Motoo Yoshimiya [a], Masato Nakatome [a], Morio Iino [a,*]

[a] Division of Forensic Medicine, Faculty of Medicine, Tottori University, Yonago 683-8503, Japan
[b] Department of Forensic Medicine & Toxicology, Jigme Dorji Wangchuk National Referral Hospital, Thimphu 11001, Bhutan
[c] Department of Mechanical Engineering, National Institute of Technology, Yonago College, Yonago 683-8502, Japan
[d] Department of Electrical Engineering & Computer Science, Faculty of Engineering, Tottori University, Tottori 680-8552, Japan

ARTICLE INFO

Keywords:
Personal identification
Age estimation
Lumbar vertebral bodies
Postmortem CT, Japanese

ABSTRACT

This study evaluated the age-related changes in the vertebral body using 3D Postmortem CT (PMCT) images and proposed an alternative age estimation formula. The PMCT images of 200 deceased individuals aged 25 to 99 years (126 males, 74 females) were retrospectively reviewed and included in the study. Using the open-source software ITK-SNAP and MeshLab, a 3D surface mesh of the fourth lumbar vertebral body (L4) and its convex hull models were created from the PMCT data. Using their inbuilt tools, volumes (in mm3) of the L4 surface mesh and convex hull models were subsequently computed. We derived VD, defined as the difference in volumes between the convex hull and L4 surface mesh normalized by L4 mesh volume, and VR, defined as the ratio of L4 mesh volume to convex hull volume based on individual L4. Correlation and regression analyses were performed between VD, VR, and chronological age. A statistically significant positive correlation ($P < 0.001$) between chronological age and VD, ($\mathbf{r}_s = 0.764$, males; $\mathbf{r}_s = 0.725$, females), and a significant negative correlation between chronological age and VR ($\mathbf{r}_s = -0.764$, males; $\mathbf{r}_s = -0.725$, females) was obtained in both sexes. The lowest standard error of the estimate was demonstrated by the VR at 11.9 years and 12.5 years for males and females, respectively. As such, their regression models to estimate adult age were Age = 248.9–2.5VR years, males; Age = 258.1–2.5VR years, females. These regression equations may be useful for estimating age in Japanese adults in forensic settings.

1. Introduction

From both the physical and forensic anthropologists' perspectives, human vertebral bodies have been explored to generate their biological profiles such as sex, age, and stature of the individual concerned. For subadults, growth-related features have been studied, whereas, for the adult population, degenerative changes observed in vertebral bodies are investigated to understand their aging patterns [1–4]. Moreover, forensic anthropologists have used normal morphological variations and comparative studies using vertebral bodies as a sole tool to obtain positive personal identification [5,6].

Vertebral osteophytes represent a gross anatomic marker of degenerative change [7]. Several methods for assessing, grading, and evaluating the osteophytes in the vertebral body have been documented for clinical and anthropological purposes [8]. Based on these osteophyte scoring systems, a few researchers have derived regression equations to estimate age [9–12]. Depending on the structural and biochemical integrity of the adjacent intervertebral disc, not only does the endplate remodel, but also transforms the whole vertebral body dimensions. Specifically, with disc degeneration, the vertical height decrease, while there is an increase in the width of the vertebral body [13,14]. As far as forensic anthropology is concerned, literature reporting on sex and stature estimation based on this vertebral morphometrics is enormous [15,16]. In contrast, there exist limited studies that have utilized this vertebral morphometrics or morphology to estimate age in the adult population.

Abbreviations: 2D, two-dimensional; 3D, three-dimensional; PMCT, postmortem CT; L4, fourth lumbar vertebral body; DICOM, digital imaging and communication in medicine; CSA, cross-sectional area; SEE, standard error of estimate; STL, stereolithography.

* Corresponding author at: Division of Forensic Medicine, Faculty of Medicine, Tottori University, 86 Nishi-Cho, Yonago, 683-8503, Japan.
E-mail address: iino@tottori-u.ac.jp (M. Iino).

https://doi.org/10.1016/j.legalmed.2023.102215
Received 3 October 2022; Received in revised form 30 January 2023; Accepted 31 January 2023
Available online 17 February 2023

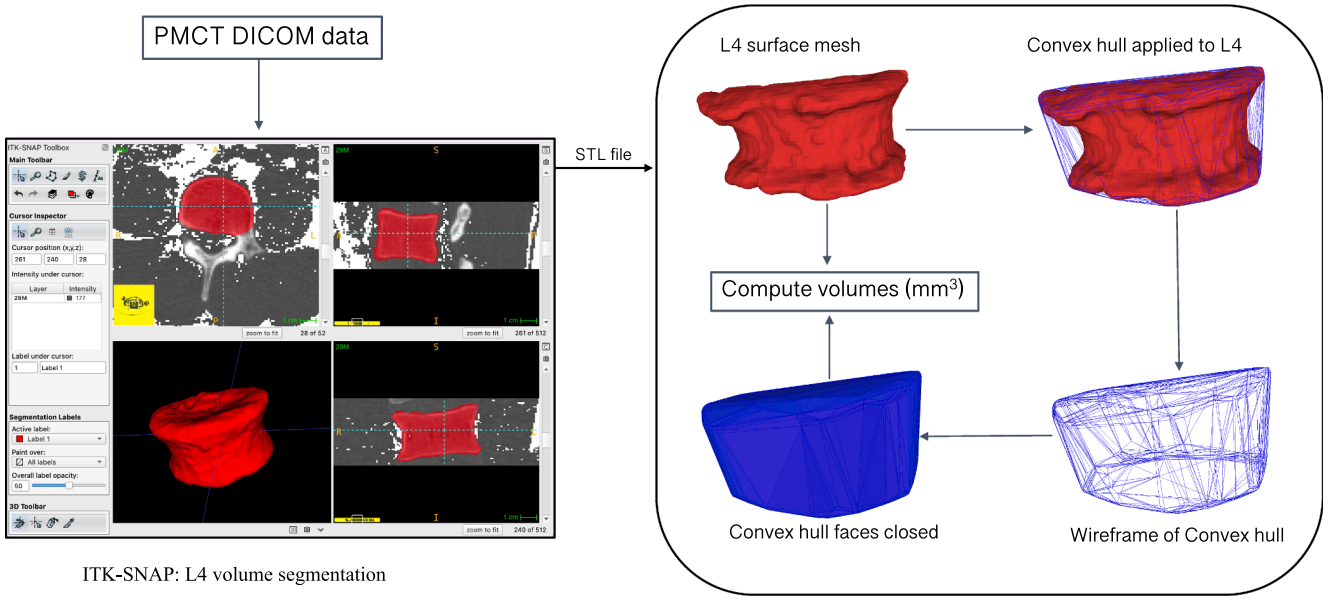

Fig. 1. Steps outlining the procedure of L4-volume segmentation in ITK-SNAP software, its surface mesh, convex-hull generation, and subsequent-volume computation in MeshLab software. DICOM: Digital Imaging and Communication in Medicine L4: Fourth lumbar vertebral body PMCT: Postmortem CT STL: Stereolithography.

Table 1
Age and sex distribution of the samples studied.

Age	Male	Female	Total
25–39	14	7	21
40–49	15	4	19
50–59	25	7	32
60–69	22	9	31
70–79	20	17	37
80–89	20	17	37
90–99	10	13	23
Total	126	74	200

Furthermore, degenerative changes and remodeling of bones occur in three dimensions (3D) [17], and estimating age using linear measurements of vertebral dimensions either in real bones or in radiographic images in two-dimensional (2D) space might under or overestimate age. Limitations such as information loss, projection errors, and misidentification of anatomical landmarks are well known in radiology when 2D techniques are applied to analyze 3D structures. However, 3D-based approaches can describe the exact location, size, and shape of bones, while also addressing issues related to image acquisition and anatomical orientations [18–20].

This study aimed to evaluate the age-related changes in the vertebral body using 3D Postmortem CT (PMCT) images and to propose an alternative age estimation formula for the adult population. Due to the maximum weight-bearing nature of the lumbar vertebral bodies, most degenerative changes are observed in them [21]. Particularly, the fourth lumbar vertebral body (L4) being farthest from the line of gravity bears the most body weight [22]. Thus, the current study was based on the 3D morphology of L4.

2. Materials and methods

The PMCT images of 200 deceased individuals with known age and sex (126 males, aged 26–99 years, mean 63 ± 18 years; 74 females, aged 25–99 years, mean 71 ± 18 years) who underwent PMCT scanning prior to forensic autopsy at the Division of Forensic Medicine, Tottori University, Japan from March 2018 to December 2021 were retrospectively reviewed and selected for this study. The study subjects included 25 years and above, and of Japanese ethnicity with known proof of birth. The vertebral ring epiphyses fuse in the mid-twenties, and its growth-related events cease subsequently [23]. Vertebral morphological changes due to endplate remodeling or osteophyte development after that are degenerative and would represent aging. Therefore, the lower limit of the age in our study samples was set at 25 years. Subjects with a history of trauma and surgeries to the vertebral column, spinal birth defects, severe burns, putrefied, and bone disease that could interfere with image interpretation were excluded. The study was approved by the Institutional Ethics Committee of Tottori University Hospital (Approval no: 22A059).

A 64-slice CT scanner, Aquilion 64 (Toshiba, Tokyo, Japan) was used to acquire the whole-body PMCT images with the following technical parameters: Tube voltage, 120 kV; tube current, 200 mA; rotation time,

Table 2
Agreement analysis between the two assessments.

Variable	First measurement		Second measurement		95 % CI	CC
	Mean	± SD	Mean	± SD		
L4 mesh vol	48109.6	7721.3	48250.9	7755.2	(0.995–0.999)	0.998
Convex hull vol	63276.4	13920.1	63520.4	14136.0	(0.993–0.999)	0.997

Volumes in mm^3.
SD standard deviation.
CI confidence interval.
CC Lin's correlation coefficient.

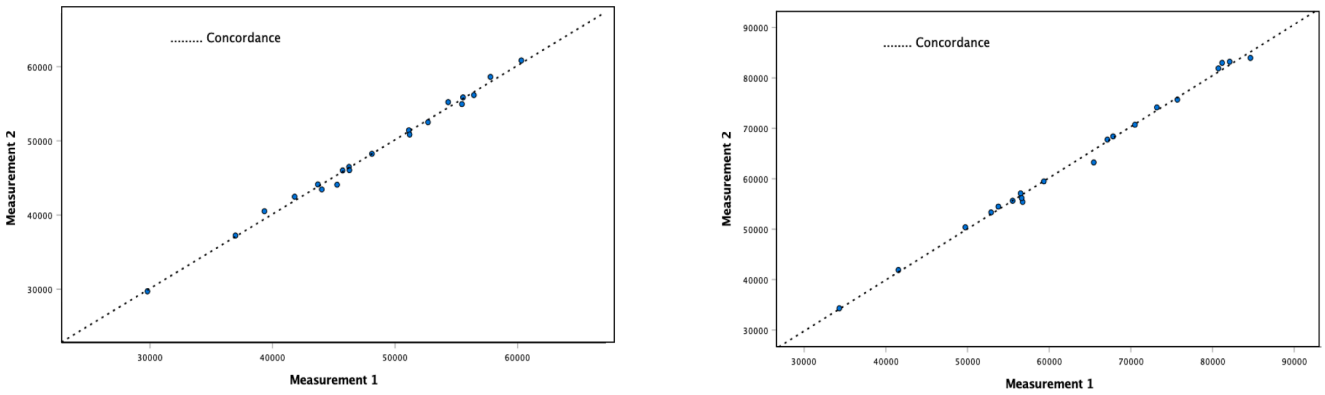

Fig. 2. Scatter plots for the mesh volume [A] and the convex hull volumes [B]. Measurements of the re-segmented mesh volume and its convex hull volumes highly correlated with their first measurement.

Table 3
Descriptive statistics of the variables between sexes.

Variables	Sex	Range	Mean ± SD	Median	P-value*
Age (years)	Male	26–99	63 ± 18	64	<
	Female	25–99	71 ± 18	75	0.001
L4 mesh vol (mm^3)	Male	29791.3–90605.6	50223.8 ± 8243.4	50764.9	= 0.001
	Female	20614.1–56744.0	37974.9 ± 7038.9	36381.7	
Convex hull vol (mm^3)	Male	34132.8–134361.5	66987.2 ± 13836.4	66353.6	< 0.001
	Female	28549.3–83352.0	50734.7 ± 11393.6	48989.6	
VD (%)	Male	15.2–57.7	32.7 ± 9.8	32.5	=
	Female	12.3–55.0	33.1 ± 9.7	31.5	0.812
VR (%)	Male	63.4–86.8	75.7 ± 5.5	75.5	=
	Female	64.5–89.0	75.5 ± 5.4	76.0	0.812

*Mann-Whitney *U* test, significant at $P < 0.05$.

Table 4
Values of VD and VR across different age groups.

Age groups	Sex	N	VD (%)		VR (%)	
			Mean	SD	Mean	SD
25–39	Male	14	20.8	2.7	82.7	1.9
	Female	7	19.1	4.1	84.0	2.9
40–49	Male	15	24.4	4.5	80.5	2.9
	Female	4	23.7	3.7	80.9	2.5
50–59	Male	25	28.8	4.9	77.7	3.0
	Female	7	28.2	3.4	78.1	2.1
60–69	Male	22	32.6	8.2	75.6	4.7
	Female	9	28.5	6.2	77.9	3.7
70–79	Male	20	39.7	9.2	71.8	4.8
	Female	17	33.4	6.5	75.1	3.5
80–89	Male	20	40.8	5.9	71.1	2.9
	Female	17	37.3	8.0	73.0	4.1
90–99	Male	10	42.1	8.6	70.6	4.3
	Female	13	43.4	8.9	70.0	4.6
P- value*	Male	126	< 0.001		< 0.001	
	Female	74	< 0.001		< 0.001	

* Kruskal-Wallis test, significant at $P < 0.05$.

1 s; collimation, 1.25 mm; and slice thickness, 1.0 mm. Raw CT data were reconstructed into 3D volumes using the standard kernel for image reconstruction using the software from the Toshiba scanner manufacturer. The 3D PMCT data were then anonymized and exported in Digital Imaging and Communication in Medicine (DICOM) format for further image processing.

2.1. L4 vertebral body segmentation and 3D surface mesh generation

ITK-SNAP software (available from https://www.itksnap.org) [24] was used to process the volumetric PMCT data and segment L4 from the DICOM files. Using the semiautomatic tool 'Active Contour Segmentation Mode' in the ITK-SNAP software, a region of interest was defined around L4, and its 3D volumetric image was segmented. A minimum threshold mode was set between 80 and 100 to separate soft tissues from the vertebral body. The pedicles, lamina, transverse processes, spinous process, and articular facets were not included in image analyses and were manually removed using the 'Paint brush' tool. The 3D volumetric image of L4 was then exported as an stereolithography (STL) file, Fig. 1.

2.2. Convex hulling and volume documentation

The STL files were imported into the open-source 3D mesh processing software MeshLab (available from https://www.meshlab.net) [25] and the 3D surface mesh of L4 were reconstructed and reviewed. Specifically, the mesh was checked for any unclosed holes. If found, it was closed using the tool "Close holes" function to make it watertight. Next, from the tool 'Remeshing, Simplification and Reconstruction' a 'Convex hull' was applied to the L4 surface mesh. In computational geometry, "the convex hull S of a set S is the smallest convex set that contains S" [26]. In our context, we described the convex hull as the smallest convex volume that has all the segmented L4 bony features. Specifically, a 3D surface mesh of L4 contains sets of vertices representing the morphology of the L4, including osteophytes, irregular endplate surface, etc. that are in X, Y, and Z coordinates. The convex hulling procedure then mounts the smallest polytope around those vertices, resulting in a close-fitting hull around the L4 surface mesh. Subsequently, the volumes (in mm^3) of the L4 surface mesh and convex hull were calculated using the inbuilt tool "Compute Geometric Measures" in MeshLab software, Fig. 1.

For each subject, we derived the following variables: L4 mesh volume, convex hull volume, volume difference (VD), and volumetric ratio (VR) based on the 3D surface mesh of individual L4. VD was calculated as the difference in volumes between the convex hull and L4 surface mesh, normalized by the volume of the L4 surface mesh as follows:

$$VD = \frac{Convex\ hull\ vol - L4mesh\ vol(mm^3)}{L4mesh\ vol(mm^3)} * 100\%$$

While VR was defined as the ratio of L4 surface mesh volume to convex hull volume, represented by the equation:

$$VR = \frac{L4mesh\ vol(mm^3)}{Convex\ hull\ vol(mm^3)} * 100\%$$

Both VD and VR were expressed as percentages and were

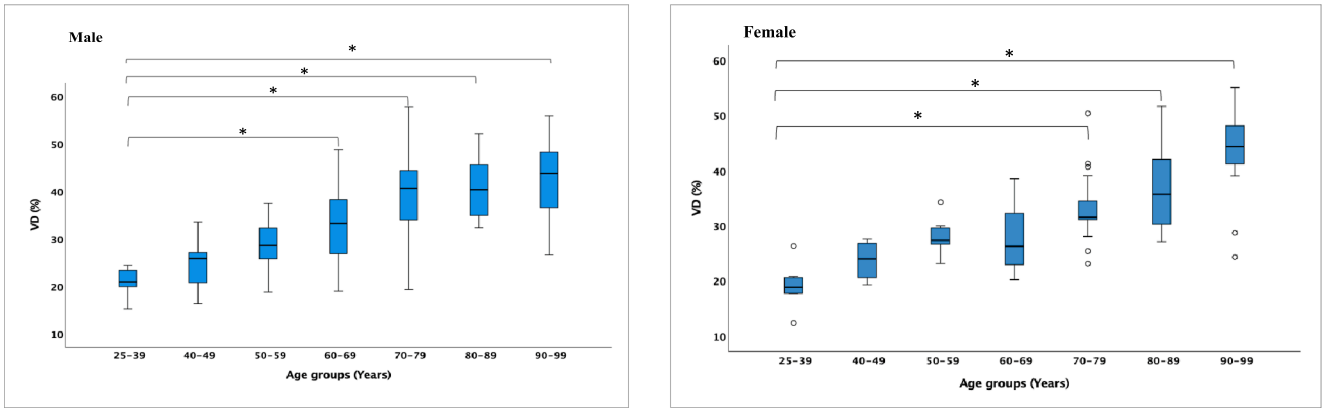

Fig. 3A. Box-and-whisker plots of the percentage VD for each age group. *Adjusted P < 0.05, Bonferroni correction. °Represent outliers.

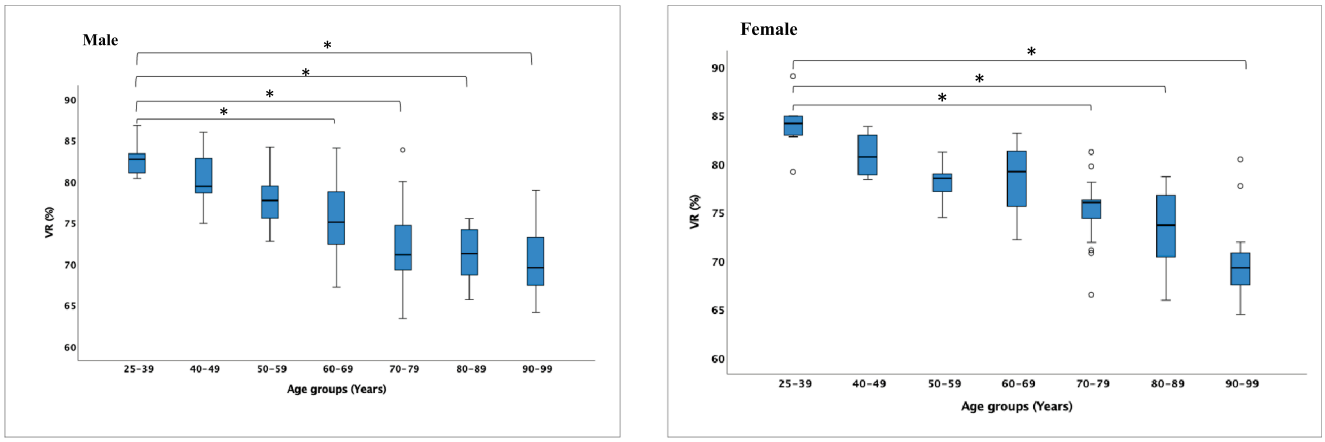

Fig. 3B. Box-and-whisker plots of the percentage VR for each age group. *Adjusted P < 0.05, Bonferroni correction. °Represent outliers.

Table 5
Spearman's r_s and regression models for estimation of chronological age (Y) from variables (X).

Sex	Variables	Spearman's r_s	Regression model	SEE	R^2	P-value
Male	L4 mesh vol	0.279	Y = 31 + 0.001X	17.241	0.086	< 0.001
	Convex hull vol	0.519	Y = 20 + 0.001X	15.670	0.245	< 0.001
	VD	0.764	Y = 18.6 + 1.4X	12.122	0.548	< 0.001
	VR	−0.764	Y = 248.9–2.5X	11.935	0.562	< 0.001
Female	L4 mesh vo	0.216	Y = 43.3 + 0.001X	17.698	0.081	= 0.014
	Convex hull vol	0.431	Y = 32.5 + 0.001X	16.232	0.227	< 0.001
	VD	0.725	Y = 26.9 + 1.3X	12.916	0.510	< 0.001
	VR	−0.725	Y = 258.1–2.5X	12.545	0.538	< 0.001

hypothesized to serve as aging indices to describe age-related morphology in L4. To assess the intra-rater agreement, one investigator re-segmented and assessed 20 PMCT images after 3 months from their first assessments.

2.3. Statistical analyses

Lin's concordance correlation coefficient (CC) was used to analyze the intra-rater agreement between the assessments [27]. The following qualitative scale was used to assess levels of concordance between the two measurements: *almost perfect* for CC greater than 0.99; *substantial* from 0.95 to 0.99; *moderate* from 0.90 to 0.95; and *poor* for CC <0.90 [28]. The normality of data was checked with the Shapiro-Wilk test. For the description of continuous data, mean and standard deviation were used. The chronological age was divided into seven age groups: 25–39 years, 40–49 years, 50–59 years, 60–69 years, 70–79 years, 80–89 years, and 90–99 years (Table 1), and the VD and VR were compared among these categories using the Kruskal-Wallis test by the sex groups (male, female). For two-group comparisons, we used the Mann-Whitey *U* test.

We also performed correlation and regression analyses among the chronological age and the variables (L4 mesh volume, convex hull volume, VD and VR). For correlation analyses, we used Spearman's correlation coefficient. Statistical analyses were performed using IBM SPSS Statistics v27. All P values quoted are 2-sided, and the significance level was set to 0.05.

3. Results

Lin's (CC) was 0.998 and 0.997 for mesh volume and convex hull volumes, respectively, which is considered a perfect agreement between the two assessments (Table 2, Fig. 2). Shapiro-Wilk test revealed that all variables (chronological age, L4 mesh volume, convex hull volume, VD, and VR) did not comply with normality for either sex (P < 0.05). Accordingly, we performed the Mann–Whitney *U* test to check for sex differences in those variables. The male subjects were significantly younger than the female (Z-value = -3.2, P < 0.001). Similarly, both L4 mesh volumes and convex hull volumes were significantly larger in

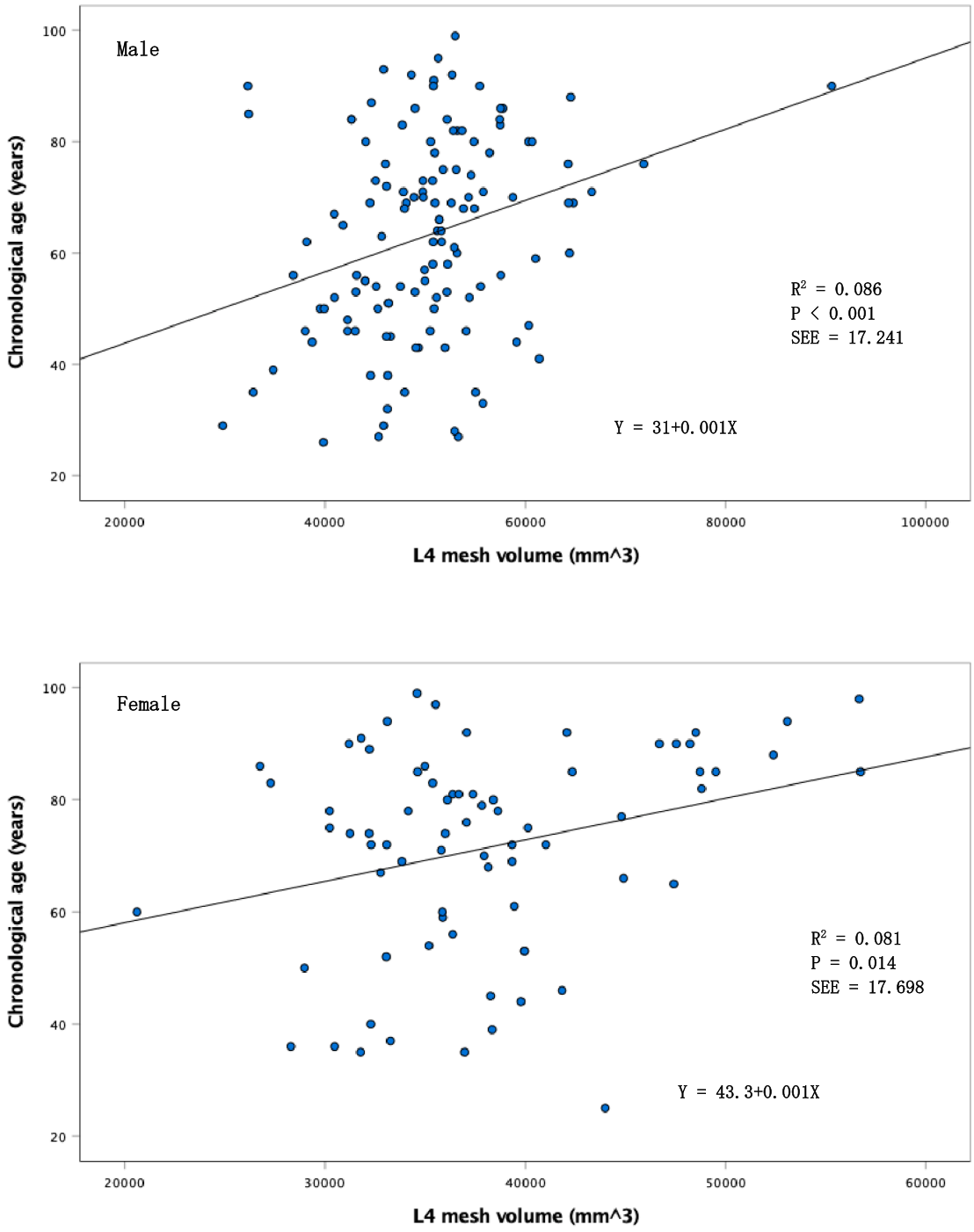

Fig. 4A. Regression lines of chronological age vs L4 mesh volumes. Note the wider inter-individual variability of mesh volumes between individuals of the same age, particularly in female subjects. R^2 = Coefficient of determination SEE = standard error of estimate.

males than in females (L4 mesh volume: Z-value = -8.86, P = 0.001; convex hull volume: Z-value = -7.84, P < 0.001). However, it was observed that values of VD and VR between the two sexes were statistically insignificant (VD: Z-value = -0.238, P = 0.812; VR: Z-value = −0.238, P = 0.812), Table 3.

The means and the standard deviation of VD and VR across different age groups are presented in Table 4. The mean VD tended to increase with age, while the mean VR tended to decrease with age in both sexes. Additionally, a Kruskal-Wallis test showed both VD and VR values significantly different among age groups in both sexes (VD: H (6) = 71.3, P < 0.001; VR: H (6) = 71.3, P < 0.001, male; VD: H (6) = 39.3, P < 0.001; VR: H (6) = 39.3, P < 0.001, female), Table 4. When pairwise comparisons with Bonferroni correction were made between age groups 25–39 and others, we found a significant difference (P < 0.05) between groups 25–39 and 60–69 (Adj. P = 0.002), between groups 25–39 and 70–79 (Adj. P < 0.001), between groups 25–39 and 80–89 (Adj. P < 0.001), and between groups 25–39 and 90–99 (Adj. P < 0.001) in males in both VD and VR. In females, there was a significant difference in VD and VR only between age groups 25–39 and 70–79 (Adj. P = 0.010), between groups 25–39 and 80–89 (Adj. P < 0.001), and between groups 25–39 and 90–99 (Adj. P < 0.001), Fig. 3.

Table 5 shows Spearman's correlation coefficient (r_s), the regression

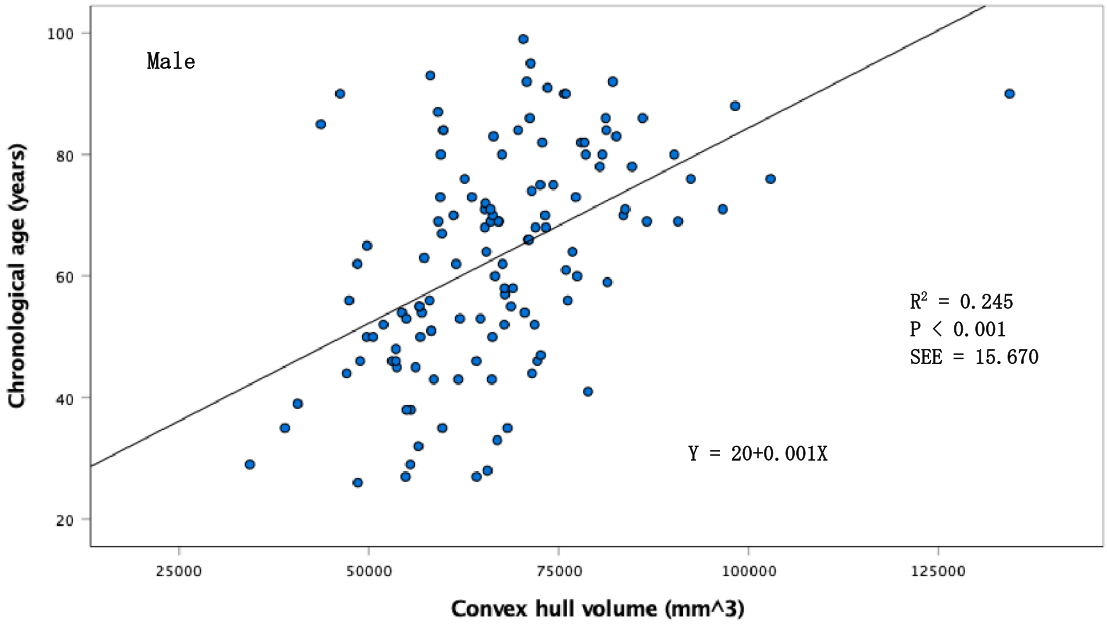

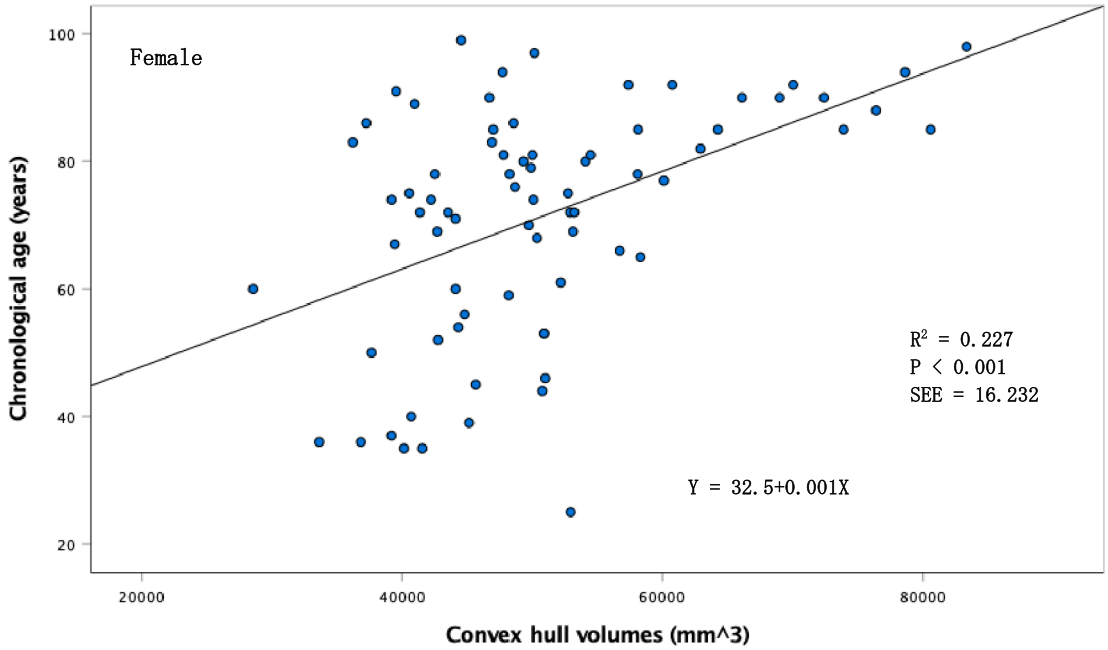

Fig. 4B. Regression lines of chronological age vs convex hull volumes. Although the correlations between the chronological age and the convex hull volumes were moderately strong and significant, their relationship with aging was not as robust as with VD and VR. R^2 = Coefficient of determination SEE = standard error of estimate.

equation, the standard error of estimate (SEE), and the coefficient of determination (R^2) obtained among the chronological age and variables. The Spearman's $\mathbf{r_s}$ obtained between chronological age and L4 mesh volume (males: $\mathbf{r_s} = 0.279$, $P = 0.002$; females: $\mathbf{r_s} = 0.216$, $P = 0.065$) and between chronological age and convex hull volume (males: $\mathbf{r_s} = 0.519$, $P < 0.001$; females: $\mathbf{r_s} = 0.431$, $P < 0.001$) were either not significant or as strong as that of the $\mathbf{r_s}$ obtained between chronological age and aging indices, VD (males: $\mathbf{r_s} = 0.764$, $P < 0.001$; females: $\mathbf{r_s} = 0.725$, $P < 0.001$); VR (males: $\mathbf{r_s} = -0.764$, $P < 0.001$; females: $\mathbf{r_s} = -0.725$, $P < 0.001$) in either sex.

The regression lines among the chronological age and the variables are shown in Fig. 4 [A-D]. Considering the SEE obtained between the chronological age and aging indices, VR showed a slightly lower SEE of 11.9 years for males (vs 12.1 years for VD), and 12.5 years for females (vs 12.9 years for VD). The regression equations generated for adult age estimation based on aging indices are as follows:

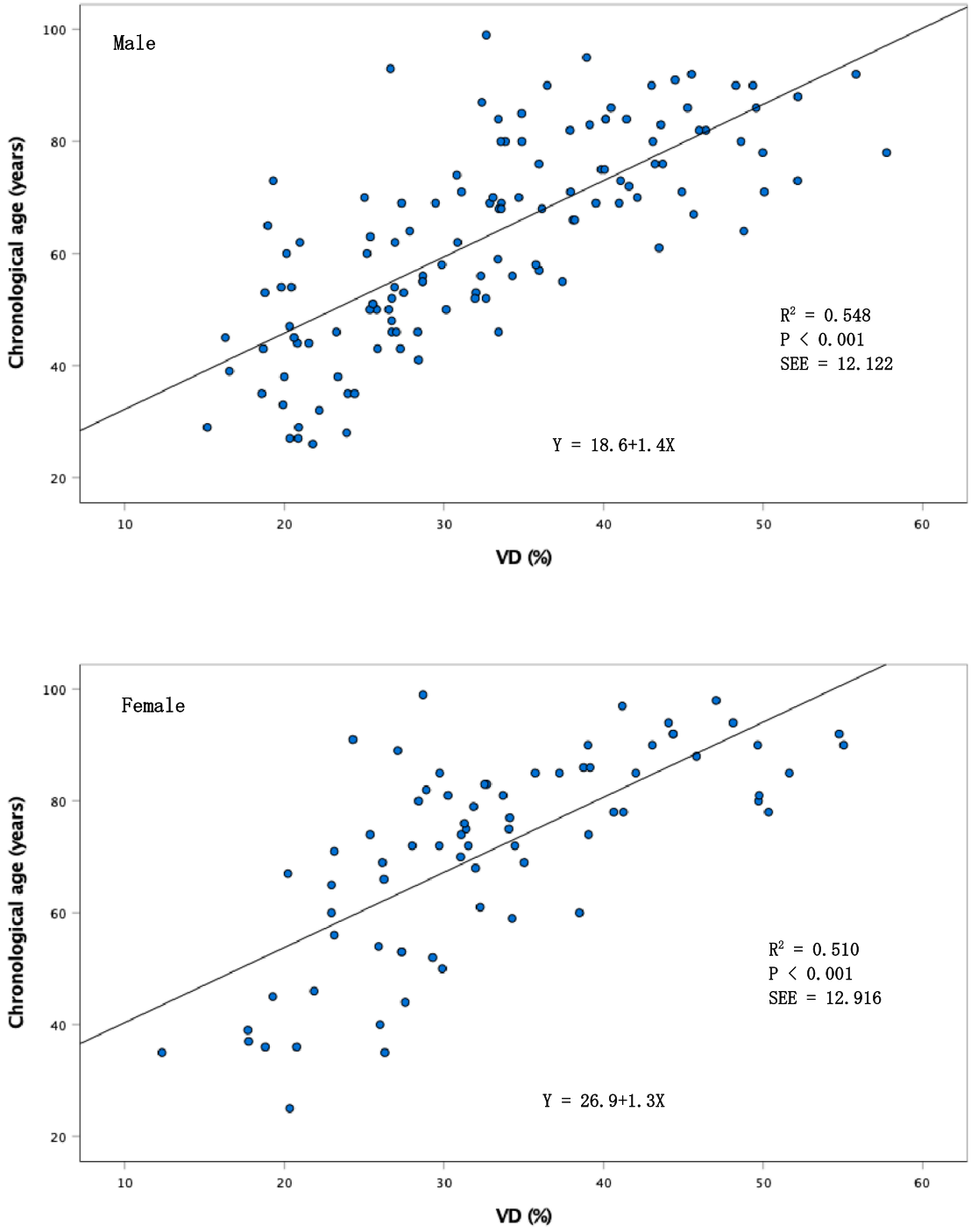

Fig. 4C. Regression lines of chronological age vs volume difference (VD). R^2 = Coefficient of determination SEE: Standard error of estimate.

For VD,
Estimated age (years): 18.6 + 1.4VD (males).
Estimated age (years): 26.9 + 1.3VD (females).
For VR,
Estimated age (years): 248.9–2.5VR (males).
Estimated age(years): 258.1–2.5VR (females).

4. Discussion

Our retrospective study conducted using 3D PMCT images was to elucidate the age-related changes in the vertebral body and to generate regression models for age estimation. The current study used a convex hulling technique to quantify and describe the 3D surface of L4. The convex hulling method has recently been used in the medical image processing fields [29–31]. Our extensive literature search of the use of the convex hull in forensic anthropology yielded only one study that used this concept. However, their study was limited to using the convex hulling technique in 2D shapes [32]. As such, this study is the first to use the convex-hulling method in a 3D space using the 3D vertebral model to study its morphology and estimate age.

The L4 mesh volumes had wider inter-individual variability even between individuals of the same age, demonstrating no appreciable relationship with aging (Fig. 4 [A]). It could be due to biological factors such as height, weight, occupation, nutrition, ethnicity, genetics, etc.,

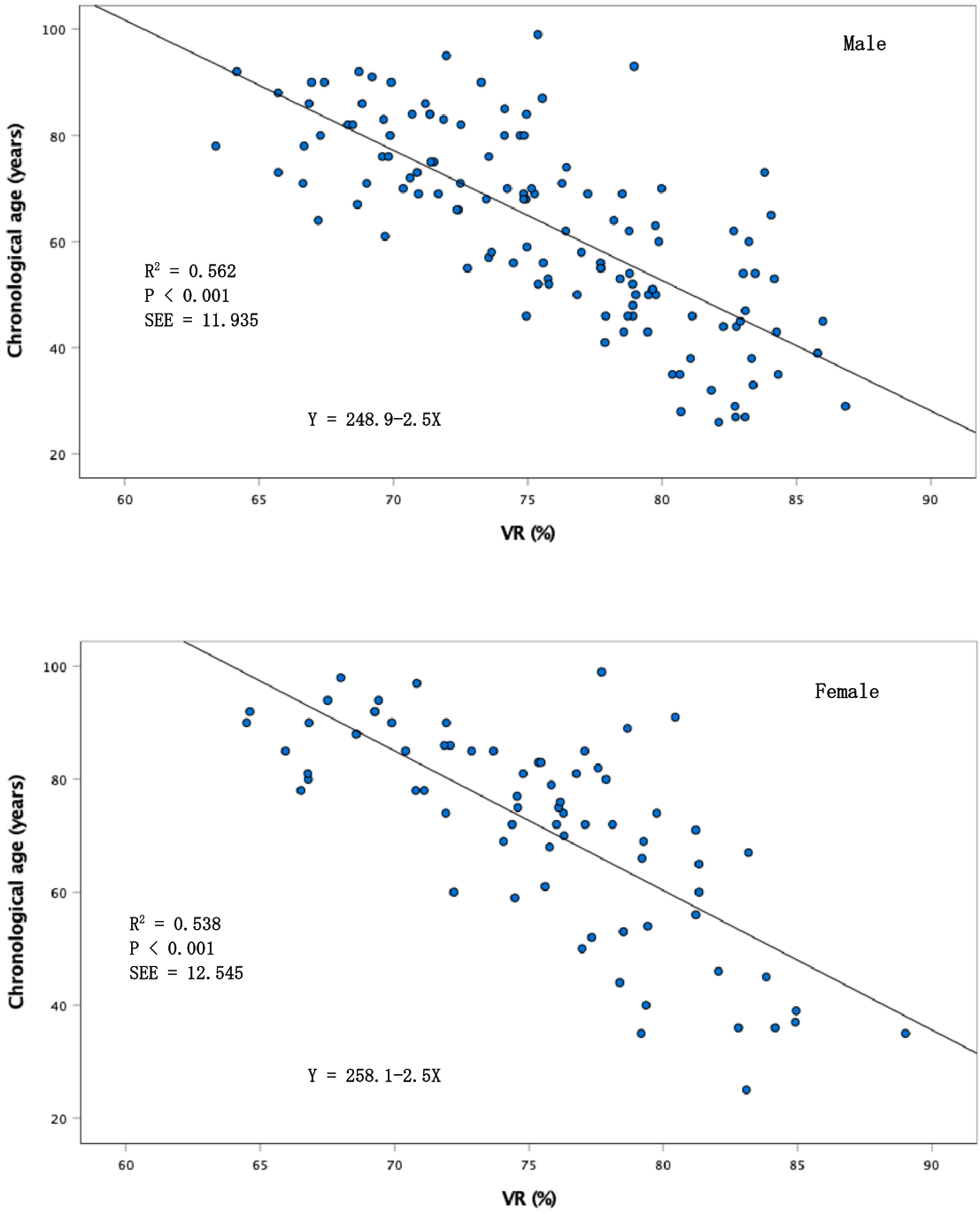

Fig. 4D. Regression lines of chronological age vs volume ratio (VR). R^2 = Coefficient of determination SEE: Standard error of estimate.

which influence the growth and anatomy of individual L4 [33]. This was also noted by Caula A et al. when they investigated the lumbar vertebral body volumes using 2D-based mathematical equations for patient morphological features. They observed that vertebral volumes mostly correlated with height and weight more than with age [34]. However, both of our studies clarified that males have larger vertebral volumes than females, which is explained by the fact that men have bigger vertebral body sizes. When the convex hull volume alone was considered for analysis, its relationship with aging was not robust (Fig. 4 [B]). The convex hull volume certainly would have overrepresented the actual deformation pattern of L4 as it includes mesh vertexes that are the farthest and form borders of the contour. Therefore, we used the volume difference and volumetric ratios of the volumes to reveal their relationships with aging. However, the normalization of the volume difference was necessary to scale the variability in vertebral volumes across the population.

The VD and VR demonstrated a linear relationship with aging, with statistically significant differences in their values among age groups, Table 4. As soon as vertebral growth ceases in the mid-twenties [23], vertebral bodies undergo various shape deformations. In a study by Junno J A et al. on the cross-sectional area (CSA) of the L4, they noted a moderate increase in CSA with age. When comparing the youngest and the oldest age groups, there was a 4%-6% increase in CSA, in both sexes. They attributed this to an increase in vertebral corpus width resulting

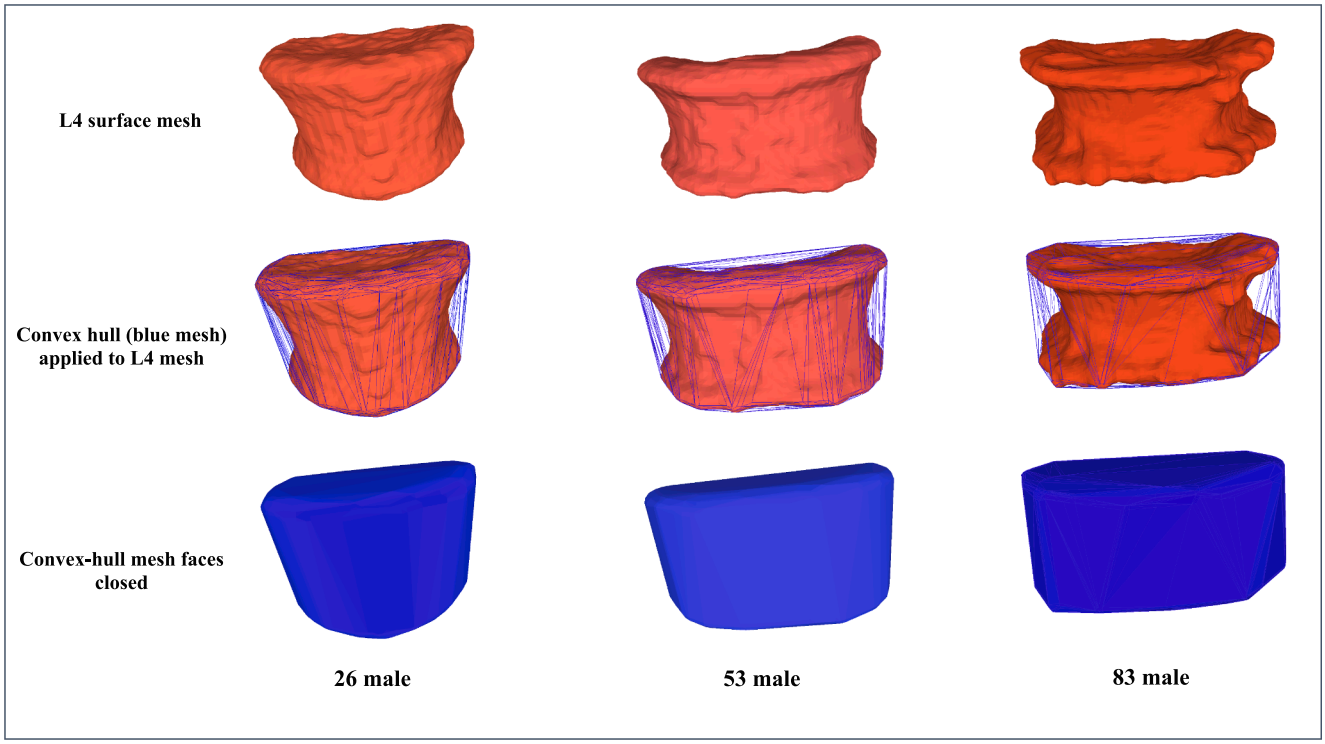

Fig. 5. Examples showing how the vertebral morphology and its corresponding convex-hull volumes change with aging.

from sub-periosteal bone deposition [22]. Whitmarsh T et al. in their study of vertebral morphometry by statistical shape analysis, evaluated various landmarks of the third lumbar vertebral body to understand their age-related changes. They noted an apparent decrease in vertebral body height, while the endplate widths increased. Notably, the lower endplate protrusion from the vertebral body was more compared with the upper endplate [35]. Indeed, the decrease in vertebral height is also not uniform; the decrease in the anterior height is more compared to the middle and posterior heights of the vertebral body, which is clinically termed wedge deformity [36]. Furthermore, the deformation process of the vertebral body is accompanied by the increased concavity of the endplate [37,38]. We hypothesized that these unequal dimensional changes and non-uniform 3D shape deformations acquired by L4 over time are represented by mesh vertexes virtually, resulting in increasing convex hull volumes, so in VD and VR with aging, as shown in Fig. 5.

We obtained a statistically significantly strong correlation between aging indices and chronological age ($P < 0.001$). Spearman's $\mathbf{r}_s$ was slightly higher in males than in females (0.764 vs 0.725) suggesting more variations in females. When these indices were regressed against the chronological age, we obtained the lowest SEE with VR (male, 11.9 years; female, 12.5 years), which is comparable to the SEE obtained from vertebral osteophyte scores [9–11]. Chiba et al. measured osteophytes of thoracic and lumbar vertebral bodies on CT images, and their scores regressed against age. They obtained a SEE of < 10 years with an R^2 of 0.8, which was slightly better than that of the current study [39]. Using vertebral diameter measurements (length, height, width, and depth), studies [40–43] have attempted to estimate adult age. However, correlations obtained from those measurements with age were not as strong as ours. Imaizumi K et al. developed an age estimation method based on machine learning using the third lumbar vertebral body, ischial tuberosity, iliac crest of the right coxal bone, and upper half of the right femur from PMCT images. They observed that the features extracted from the third lumbar vertebral body obtained the highest accuracy in males, whilst ischial tuberosity demonstrated the highest accuracy in females in one of the machine learning algorithms employed [44]. The method presented objectivity, automation, and accuracy, but their automatic feature extraction was based on 2D images of the given bones.

Despite several methodologies adopted to estimate adult age from the vertebral bodies, there remains an issue of a wide prediction age range. Unlike in the subadult population, where growth-related features are more uniform, degenerative changes in adult bones are highly variable, as demonstrated by a wider range of values in this study (Fig. 4). However, it is to be noted that the current age estimation was based on L4 alone, and if other or several vertebral bones were considered for analysis, our technique might have outperformed the existing age estimation techniques. As mentioned earlier, besides osteophyte development, spectrums of morphological changes occur in the aging vertebral body, such as endplate remodeling, vertebral diameter change, and volumetric alteration. Estimating age using osteophyte evaluation alone would not be sufficient as it would be based on a 'one bony feature' analysis. As such, the proposed age estimation method represents a systematic approach that includes all these degenerative features, from a 3D perspective, and is easier to compute.

Our study has several limitations. One major limitation is that there was a possibility of introducing errors while segmenting the L4 vertebral body and measuring its mesh and convex hull volumes. Although the intra-rater agreement analyses confirmed its reproducibility, we couldn't include the inter-rater agreement analyses in the current work. We acknowledge that a second investigator segmenting and repeating the whole process would have provided a better evaluation of the reproducibility of the method proposed. Another limitation of this study is there were very few study samples in the lower age groups, especially those below 40 years. Being retrospective and descriptive, this study depended only on the existing samples in the PMCT database which unfortunately had fewer samples in younger age groups. Furthermore, in the current study, we have not considered biological parameters such as body weight, stature, occupation, nutrition, etc., of the individuals for possible interactions that would have influenced the overall results. More importantly, regression equations derived in this study would apply only to the adult Japanese population. Further studies are needed to validate the proposed method with a larger sample size, using different vertebral bones, alone or in combinations, and from different

population backgrounds.

5. Conclusion

Using 3D PMCT images of L4, we could describe its age-related changes and propose an alternative methodology to estimate adult age in Japanese. The technique was based on L4 surface mesh generation and the subsequent convex-hulling process in 3D space. The volumes computed from the digital models were then used to derive aging indices, VD, and VR. VD showed a significantly positive correlation with age, while VR negatively correlated with age. The lowest standard error of the estimate was demonstrated by the VR at 11.9 years and 12.5 years for males and females, respectively. As such, their regression models to estimate age were Age = 248.9–2.5VR years for males; Age = 258.1–2.5VR years for females.

Funding

This research did not receive any specific grant from funding agencies in the public, commercial, or not-for-profit sectors.

Ethical approval

The study was approved by the Institutional Ethics Committee of Tottori University Hospital (Approval no: 22A059).

Declaration of Competing Interest

The authors declare that they have no known competing financial interests or personal relationships that could have appeared to influence the work reported in this paper.

References

[1] J.J. Snodgrass, Sex Differences and Aging of the Vertebral Column, J Forensic Sci. 49 (2004) 458–463. PMID: 15171159.
[2] A. Klein, K. Nagel, J. Gührs, C. Poodendaen, K. Puschel, M.M. Morlock, et al., On the relationship between stature and anthropometric measurements of lumbar vertebrae, Sci Justice 55 (2015) 383–387, https://doi.org/10.1016/j.scijus.2015.05.004.
[3] A. Azofra-Monge, A. Aguilera, Morphometric research and sex estimation of lumbar vertebrae in a contemporary Spanish population, Forensic Sci Med Pathol. 16 (2020) 216–225, https://doi.org/10.1007/s12024-020-00231-6.
[4] Y.-K. Choi, J. Kim, T. Yamaguchi, K. Maki, C. Chang Ko, Y.I. Kim, Predicting the Skeletal Maturation Stages, BioMed Research International 2016 (2016), https://doi.org/10.1155/2016/8696735.
[5] L. Watamaniuk, T. Rogers, Positive Personal Identification of Human Remains Based on Thoracic Vertebral Margin Morphology, J Forensic Sci. 55 (5) (2010) 1162–1170, https://doi.org/10.1111/j.1556- 4029.2010.01447.x.
[6] A.Z. Mundorff, G. Vidoli, J. Melinek, Anthropological and Radiographic Comparison of Vertebrae for Identification of Decomposed Human Remains, J Forensic Sci. 51 (5) (2006) 1002–1004, https://doi.org/10.1111/j.1556-4029.2006.00233. x.
[7] Z. Klaassen, R.S. Tubbs, N. Apaydin, R. Hage, R. Jordan, M. Loukas, Vertebral spinal osteophytes, Anat Sci Int. 86 (1) (2011) 1–9, https://doi.org/10.1007/s12565-010-0080-8.
[8] S. Praneatpolgrang, S. Das, P.M.P. Navic, Age-Related Changes in the Vertebral Osteophytes: A Review, Int Med J. 27 (2020) 181–184.
[9] S. Watanabe, K. Terazawa, Age estimation from the degree of osteophyte formation of vertebral columns in Japanese, Leg Med. 8 (2006) 156–160, https://doi.org/10.1016/j.legalmed.2006.01.001.
[10] S. Praneatpolgrang, S. Prasitwattanaseree, P. Mahakkanukrauh, Age estimation equations using vertebral osteophyte formation in a Thai population: Comparison and modified osteophyte scoring method, Anat Cell Biol. 52 (2019) 149–160, https://doi.org/10.5115/acb.2019.52.2.149.
[11] G.A. Listi, M.H. Manhein, The Use of Vertebral Osteoarthritis and Osteophytosis in Age Estimation, J Forensic Sci. 57 (2012) 1537–1540, https://doi.org/10.1111/j.1556-4029.2012.02152. x.
[12] E. Kacar, E. Unlu, M. Beker-Acay, C. Balcik, M.A. Gultekin, U. Kocak, et al., Age estimation by assessing the vertebral osteophytes with the aid of 3D CT imaging, Australian Journal of Forensic Sciences 49 (2017) 449–458, https://doi.org/10.1080/00450618.2016.1167241.
[13] M. Benoist, Natural history of the aging spine, Eur Spine J. 12 (Suppl 2) (2003) S86–S89, https://doi.org/10.1007/s00586-003-0593-0.
[14] S.V. Kushchayev, T. Glushko, M. Jarraya, K.H. Schuleri, M.C. Preul, M.L. Brooks, O. M. Teytelboym, ABCs of the degenerative spine, Insights Imaging 9 (2) (2018) 253–274, https://doi.org/10.1007/s13244-017-0584.
[15] A. Rohmani, M.S. Shafie, F.M. Nor, Sex estimation using the human vertebra: a systemic review, Egypt, J Forensic Sci. 11 (25) (2021), https://doi.org/10.1186/s41935-021-00238-2.
[16] C.L. Choong, A. Alias, R. Abas, Y.S. Wu, J.Y. Shin, Q.F. Gan, et al., Application of anthropometric measurements analysis for stature in human vertebral column: A systematic review, Forensic Imaging 20 (2020), https://doi.org/10.1016/j.fri.2020.200360.
[17] H. Biwasaka, Y. Aoki, Y. Takahashi, M. Fukuta, A. Usui, Y. Hosokai, et al., A quantitative morphological analysis of three-dimensional CT coxal bone images of contemporary Japanese using homologous models for sex and age estimation, Leg Med. 36 (2019) 1–8, https://doi.org/10.1016/j.legalmed.2018.09.017.
[18] R. Nalçaci, F. Öztürk, O. Sökücü, A comparison of two-dimensional radiography and three dimensional computed tomography in angular cephalometric measurements, Dentomaxillofacial Radiol. 39 (2010) 100–106, https://doi.org/10.1259/dmfr/82724776.
[19] D.J. Halazonetis, From 2-dimensional cephalograms to 3-dimensional computed tomography scans, Am J Orthod Dentofac Orthop. 127 (2005) 627–637, https://doi.org/10.1016/j.ajodo.2005.01.004.
[20] R. Setiawati, P. Rahardjo, I. Ruriana, G. Guglielmi, Anthropometric study using three-dimensional pelvic CT scan in sex determination among adult Indonesian population, Forensic Sci Med Pathol. (2022), https://doi.org/10.1007/s12024-022-00526-w.
[21] L.T. Pedersen, K. Domett, Adult age at death estimation: methods tested on Thai postcranial skeletal remains, Anthropol Sci. 130 (2022) 147–159, https://doi.org/10.1537/ase.211219.
[22] J.A. Junno, M. Paananen, J. Karppinen, J. Niinimäki, M. Niskanen, H. Maijanen, et al., Age-related trends in vertebral dimensions, J Anat. 226 (2015) 434–439, https://doi.org/10.1111/joa.12295.
[23] M. Albert, D. Mulhern, M.A. Torpey, E. Boone, Age estimation using thoracic and first two lumbar vertebral ring epiphyseal union, J Forensic Sci. 55 (2010) 287–294, https://doi.org/10.1111/j.1556-4029.2009.01307. x.
[24] P.A. Yushkevich, J. Piven, H.C. Hazlett, R.G. Smith, S. Ho, J.C. Gee, et al., User-guided 3D active contour segmentation of anatomical structures: Significantly improved efficiency and reliability, Neuroimage 31 (2006) 1116–1128, https://doi.org/10.1016/j.neuroimage.2006.01.015.
[25] Cignoni P, Callieri M, Corsini M, Dellepaine M, Ganovelli F, Ranzuglia G, MeshLab: An open- source mesh processing tool. 6th Eurographics Ital Chapter Conf. Salerno, Italy (2008) 129–136.
[26] De Berg M, Cheong O, Van Kreveld M, Overmars M, Computational geometry: Algorithms and applications, Springer Berlin Heidelberg (2008). DOI: 10.1007/978-3-540-77974-2.
[27] L.I. Lin, A concordance correlation coefficient to evaluate reproducibility, Biometrics 45 (1989) 255–268, https://doi.org/10.2307/2532051.
[28] L.I. Lin, G. McBride, J.M. Bland, D.G. Altman, A proposal for strength-of-agreement criteria for Lin's Concordance Correlation Coefficient, NIWA Client Rep 45 (2005) 307–310.
[29] Y. Wang, Z. Xiong, A. Nalar, B.J. Hansen, S. Kharche, G. Seemann, et al., A robust computational framework for estimating 3D Bi-Atrial chamber wall thickness, Comput Biol Med. 114 (2019), https://doi.org/10.1016/j.compbiomed.2019.103444.
[30] M. Yadollahi, A. Procházka, M. Kašparová, Vysata, Mark V, Separation of overlapping dental arch objects using digital records of illuminated plaster casts, Biomed Eng Online 14 (2015), https://doi.org/10.1186/s12938-015-0066-9.
[31] J.N. Stember, J. Newhouse, G. Behr, S. Alam, A Convex Hull-Based New Metric for Quantification of Bladder Wall Irregularity in Pediatric Patients with Congenital Anomalies of the Kidney and Urinary Tract, J ultrasound Med. 36 (2017) 2203–2208, https://doi.org/10.1002/jum.14270.
[32] Prieto J, Mihaila S, Hilaire A, Fanton L, Odet C, Revol-Muller C, Age estimation from 3D X-ray CT images of human fourth ribs, Proceedings of the International Conference on Image Processing, Computer Vision, and Pattern Recognition (IPCV), Las Vegas, NV, USA, 16–19 July (2012) p. 1.
[33] L.A. Zukowski, A.B. Falsetti, M.D. Tillman, The influence of sex, age and BMI on the degeneration of the lumbar spine, J Anat 220 (2012) 57–66, https://doi.org/10.1111/j.1469-7580.2011.01444. x.
[34] A. Caula, G. Metmer, E. Havet, Anthropometric approach to lumbar vertebral body volumes, Surgical and Radiologic Anatomy 38 (2016) 303–308, https://doi.org/10.1007/s00276-015-1552-2.
[35] T. Whitmarsh, L.M.D.R. Barquero, S.D. Gregorio, J.M. Sierra, L. Humbert, et al., Age-Related Changes in Vertebral Morphometry by Statistical Shape Analysis, Lecture Notes in Computer Science (2012) 30–39, https://doi.org/10.1007/978-3-642-33463-4_4.
[36] K.H. Kim, J.Y. Park, S.U. Kuh, D.K. Chin, K.S. Kim, Y.E. Cho, Changes in spinal canal diameter and vertebral body height with age, Yonsei Med J. 54 (2013) 1498–1504, https://doi.org/10.3349/ymj.2013.54.6.1498.
[37] Louie PK, Orías AAE, Fogg LF, laBelle M, An HS, Anderssson GBJ, et al., Changes in lumbar endplate area and concavity associated with disc degeneration, Spine (Phila Pa 1976) 43 (2018) E1127–E1134. DOI: 10.1097/BRS.0000000000002657.
[38] T. Singh, W.C.H. Parr, W.J. Choy, G.R. Budiona, M. Maharaj, X. Mathis, et al., Three-Dimensional Morphometric Analysis of Lumbar Vertebral End Plate Anatomy, World Neurosurg. 135 (2020) e321–e332, https://doi.org/10.1016/j.wneu.2019.11.158.
[39] F. Chiba, G. Inokuchi, Y. Hoshioka, A. Sakuma, Y. Makino, S. Torimitsu, et al., Age estimation by evaluation of osteophytes in thoracic and lumbar vertebrae using postmortem CT images in a modern Japanese population, Int J Legal Med. 136 (2022) 261–267, https://doi.org/10.1007/s00414-021- 02714-9.
[40] R. Jankauskas, Variability of vertebral column measurements in Lithuanian paleopopulation, Int J Anthropol. 9 (1994) 137–151, https://doi.org/10.1007/BF02447602.

[41] N. Ramadan, S.MH.A. El, A.F. Hanon, N.F. El-Sayed, A.Y. Al-Amir, Age and Sex Identification Using Multi-slice Computed Tomography of the Last Thoracic Vertebrae of an Egyptian Sample, J Forensic Res. 08 (2017), https://doi.org/10.4172/2157-7145.1000386.

[42] A. Gulec, B.K. Kacira, H. Kütahya, H. Ozbiner, M. Ozturk, C.S. Solbas, et al., Morphometric analysis of the lumbar vertebrae in the Turkish population using three-dimensional computed tomography: Correlation with sex, age, and height, Folia Morphol. 76 (2017) 433–439, https://doi.org/10.5603/FM. a2017.0005.

[43] S.R. Saadat Mostafavi, A. Memarian, O. Motamedi, M.M. Nejad Khanamani, M. Khaleghi, S. Hbibi, Fourth lumbar vertebral parameters in predicting the gender, height and age in Iranian population, Forensic Sci Int Reports 3 (2021), https://doi.org/10.1016/j.fsir.2021.100175.

[44] K. Imaizumi, S. Usui, K. Taniguchi, Y. Ogawa, T. Nagata, K. Kaga, et al., Development of an age estimation method for bones based on machine learning using post-mortem computed tomography images of bones, Forensic Imaging 26 (2021), https://doi.org/10.1016/j.fri.2021.200477.